JOURNAL OF MATERIALS PROCESSING TECHNOLOGY XXX (2008) XXX–XXX

journal homepage: www.elsevier.com/locate/jmatprotec

Effect of starch filler content and sintering temperature on the processing of porous 3Y–ZrO_2 ceramics

L.B. Garrido[a,*], *M.P. Albano*[a], *K.P. Plucknett*[b], *L. Genova*[c]

[a] *CETMIC Centro de Tecnología de Recursos Minerales y Cerámica (CIC-CONICET-UNLP), Cam. Centenario y 506, C.C.49 (B 1897 ZCA) M.B. Gonnet, Buenos Aires, Argentina*

[b] *Department of Process Engineering and Applied Science, Dalhousie University, 1360 Barrington Street, Halifax, Nova Scotia, B3J 1Z1 Canada*

[c] *IPEN Instituto de Pesquisas Energéticas e Nucleares, CCTM Centro de Ciência e Technologia de Materiais, Cidade Universitária, Travessa R 400, 05508-900 São Paulo, Brazil*

ARTICLE INFO

Article history:
Received 12 July 2007
Received in revised form
11 February 2008
Accepted 20 February 2008

Keywords:
Zirconia
Porous 3Y–ZrO_2
Starch consolidation
Colloidal processing

ABSTRACT

A direct casting process was used to produce porous 3Y–ZrO_2 ceramics using starch as a fugitive filler and binder. The compositions with low additions of starch had higher porosity than the volume fraction of starch initially in the green body (X_{st}), whereas, the compositions with high amounts of starch produced lower porosity than the predicted value. The well ordered structure consisted of spherical pores of 8–10 μm diameter, retained from the original starch particles, connected by channels. The interconnection between pores was dependent on the volume fraction of starch incorporated, as well as on the sintering temperature. Pore interconnection was observed for all the compositions sintered at 1000–1300 °C. Increasing the sintering temperature to 1400–1500 °C produced a marked dependence of the open to total porosity ratio on X_{st}. For a high porosity material, a bimodal channel size distribution was found at 1400 and 1500 °C. The primary pore channel diameter was 0.7 μm and the secondary one was close to 4 μm. As the sintering temperature increased, the volume of the connecting channels decreased; at 1500 °C only a minor volume of the larger channels was found.

1. Introduction

The use of porous ceramics has continually increased for high temperature applications, conditions where chemical stability and good corrosion resistance are required (Saggio-Woyansky et al., 1992; Studart et al., 2006). In particular, the preparation of porous zirconia had received much attention due to its extensive industrial applications: ceramic filters (Zender et al., 1990); catalyst supports and membranes for gas filtration (Deng et al., 2002, 2003), solid oxide fuel cells (Gu et al., 1999; Boaro et al., 2003), biological materials (Rambo et al., 2004), etc.

The simplest approach to fabricate porous ceramics involves partial sintering (Deng et al., 2002, 2003) which develops a fine pore structure (Diaz et al., 2005). Alternatively, various processing techniques are available to enhance porosity, or to obtain a controlled pore size and porosity in ceramic bodies, depending on the specific application. A common processing method involves pressing a powder mixture of ceramic particles and pore forming agents, with the pore former subsequently eliminated during heating. In this way, porous ceramics of zirconia (Luo and Stevens, 1999; Diaz et al., 2005) as well as semiconducting $BaTiO_3$ (Kim et al., 2004) and silicon nitride (Diaz and Hampshire, 2004) have been prepared.

* *Corresponding author.*
E-mail addresses: lgarrido@cetmic.unlp.edu.ar, garridol@netverk.com.ar (L.B. Garrido).
0924-0136/$ – see front matter © 2008 Elsevier B.V. All rights reserved.
doi:10.1016/j.jmatprotec.2008.02.074

Pore forming agents are usually organic particles (e.g. carbon, synthetic polymers, polysaccharides, etc.) which decompose easily on heating at relatively low temperatures (Studart et al., 2006).

Starch is a low cost pore former that can simultaneously act as a binder during the formation of ceramics by a starch consolidation casting method (Lyckfeldt and Ferreira, 1998). This simple method was used to prepare many complex shaped bodies of alumina (Lyckfeldt and Ferreira, op cit. and Gregorova et al., 2006a,b) including cordierite (Alves et al., 1998), calcium carbonate (Lemos and Ferreira, 2000), mullite (Barea et al., 2005); silicon nitride (Diaz and Hampshire, 2004; Diaz et al., 2005). Most materials showed macroporous ($\geq$50 μm) structures. These studies and recently Gregorova and Pabst (2007) reported that morphology and the size of pores are specific to the type of starch used to create the porosity. The porosity of a sintered body with an added pore former can be compared with the volume fraction of the pore former relative to the volume of the green compact, the X_{pf} parameter. According to Slamovich and Lange (1992) an estimation of X_{pf} is obtained using the following expression:

$$X_{pf} = \frac{\phi(\rho z)}{1 - \phi + (\rho z)\phi} \quad (1)$$

where ϕ is the volume of organic inclusions (pore former) with respect to the volume of solids, and ρz is the relative packing density of the ceramic particles in the green compact without added inclusions. Thus, X_{pf} depends on the packing density of the ceramic particles in the green compact.

Eq. (1) considers that the large pores left by the organic inclusions shrink by the same amount as the surrounding matrix during sintering. Slamovich and Lange (1992) showed that large pores persist even after prolonged sintering times. Thus, the porosity in the sintered body (with full densification of the matrix) be nominally identical to X_{pf} in the green body.

The porosity change with addition of starch as a pore former showed good agreement with the volume of starch in the dried compact, X_{st}, calculated by Eq. (1) as previously reported for (Luo and Stevens, 1999; Diaz and Hampshire, 2004). However, the starch consolidation casting includes a heating step of the starch granules in water within the gelation temperature range (i.e. 60–80 °C). The starch granules absorb water and irreversibly swell to several times their initial size (Fennema, 1996). Then, the swollen granules will begin to rupture and collapse. Thus, a viscous dispersion of granule fragments and dissolved molecules may finally become a viscous starch solution. The gel that is formed may be considered as a composite made by swollen gelatinized granules of mainly amylopectin, dispersed in an amylose gel matrix (Rosalina and Bhattacharya, 2002; Pabst et al., 2002). Thus, porosity formation with starch consolidation casting is different from that of porous materials prepared without gelling the starch (Gregorova et al., 2006b). Therefore, as a first study, a comparison between predicted porosity with Eq. (1) and the total porosity of the sintered ceramic prepared by starch consolidation may be a measure of the deviation that exists.

In the present work, porous zirconia ceramics were produced by a starch consolidation process (Lyckfeldt and Ferreira, 1998), which involves the preparation of a concentrated zirconia suspension with added corn starch. The efficiency of the dispersion process on the packing of the ceramic particles as well as the relative density, drying shrinkage of green compacts were examined. In addition, the influence of the volume fraction of starch filler, and the sintering temperature on the densification behavior and microstructure, will be discussed.

2. Experimental

2.1. Materials and methods

A commercial zirconia powder doped with 3 mol% yttria (YZ01, Saint-Gobain, France) was used in this study, subsequently referred to as 3Y–ZrO_2. The mean particle diameter and the specific surface area were 0.6 μm and 7 m^2/g, respectively. Corn starch, commercially available in Argentina, was used as pore former agent and binder. Experiments were carried out using the as-received starch, without any subsequent processing. The average size of the spherical granule of starch was approximately 10 μm. A commercial ammonium salt of a polycarboxylic acid (Dolapix CE64, Zschimmers and Schwartz, Germany) was used as a dispersant.

2.2. Suspension preparation

Concentrated aqueous 3Y–ZrO_2 suspensions, with solids loading from 78 to 85 wt.%, were prepared by deagglomeration of the powder in distilled water with different amounts of dispersant at pH 9 using an ultrasonic bath. Different amounts of starch in a range of 16–60 wt.% (dry weight basis of 3Y–ZrO_2 powder), were added to the stabilized 3Y–ZrO_2 suspensions followed by ultrasonic treatment. The resultant volume fraction of starch (ϕ) varied between 0.40 and 0.71. The water content of the suspension was experimentally adjusted in order to obtain a fluid suspension and to gel the starch. The total solids loading of the suspensions was set to 52–55 vol.%.

2.3. Preparation of green compact

The consolidation of the suspensions was performed in a covered mold, which was coated with a release agent, at 90 °C for 30 min. The starch particles swell by water uptake from the slip, causing the ceramic particles to stick together and, consequently, consolidate into a solid body. The resulting compacts were left in the mold at room temperature; after slight drying shrinkage occurred, the samples were de-molded. The samples, with approximate dimensions of 25 mm diameter and 15–20 mm thickness, were then dried at 100 °C until there was no further change in mass. 3Y–ZrO_2 compacts without starch were also prepared by slip casting in a plaster mold. The cast samples were dried at room temperature and then at 100 °C.

2.4. Pre-calcination and sintering

The burning out of starch was achieved by slow heating up to 1000 °C with three isothermal hold steps at 150, 250 and 300 °C; the samples were then held for 2 h at 1000 °C. The pre-calcined cylinders were then sintered at 1300, 1400 or 1500 °C

Please cite this article in press as: Garrido, L.B., et al., Effect of starch filler content and sintering temperature on the processing of porous 3Y–ZrO_2 ceramics, J. Mater. Process. Tech. (2008), doi:10.1016/j.jmatprotec.2008.02.074

for 2 h, using a heating rate of 5 °C/min. The 3Y–ZrO_2 green compacts prepared without starch were also sintered at these three temperatures.

2.5. *Characterization of green and sintered compacts*

The density of green compacts was measured by Hg immersion. The relative sintered density (RD) and open porosity were determined by the water absorption method. A density of 6.05 and 1.45 g/cm^3 were used for 3Y–ZrO_2 and starch, respectively.

The mean pore radius and the pore size distribution, characterizing the interconnecting pores between the large ones left by the starch granules, were determined for sintered compacts using Hg porosimetry (Carlo Erba Porosimeter 2000, Italy). The microstructure of the dried and sintered samples were observed on fracture surfaces using a field emission scanning electron microscope (FE-SEM) (Model S-4700, Hitachi High Technologies Corporation, Japan).

3. Results and discussion

3.1. *Effect of dispersant addition on the green density of 3Y–ZrO_2 prepared with 0.45 vol.% starch*

Fig. 1 shows the relative density of green compacts, with and without starch, as a function the dispersant concentration. For the 3Y–ZrO_2 compacts without starch, a maximum in the green density (62% TD) was obtained at a polyelectrolyte concentration of about 0.20 wt.%, which was an effective amount to stabilize the 3Y–ZrO_2 suspensions. The high degree of dispersion of 3Y–ZrO_2 particles is related to the polyelectrolyte adsorption on the powder surface. The decrease in the green density at dispersant concentration lower and higher than 0.20 wt.% was attributed to flocculation.

The compacts with starch showed a maximum at nearly the same dispersant concentration when compared to the compacts without starch. This result indicated that the dispersion of 3Y–ZrO_2 particles was not affected by the presence

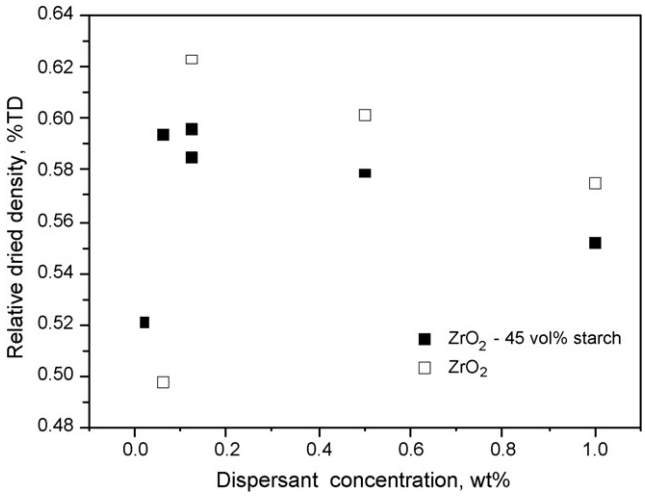

Fig. 1 – Relative density of green compacts with and without starch, as a function of the dispersant concentration.

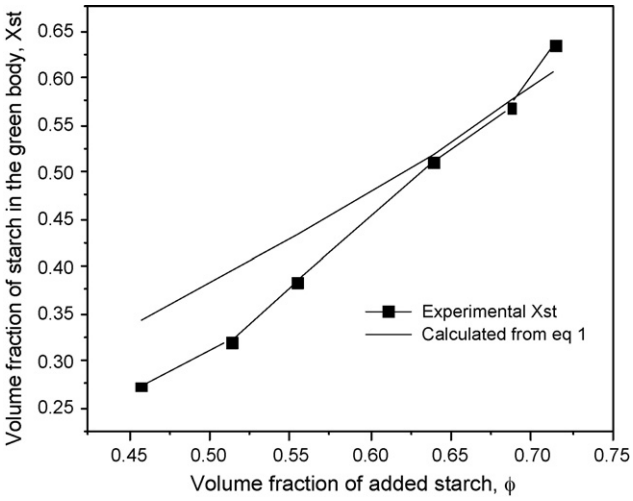

Fig. 2 – Volume fraction of starch in the green body (X_{st}) as a function of the volume fraction of added starch φ.

of starch in the suspension using the polyelectrolyte as dispersant. The chemical structure of starch consists of mixtures of two polysaccharide types, one that is linear, amylose, and one that is highly branched, amylopectin. The glucose units that comprise the polymeric chains in starch expose a large number of terminal hydroxyls groups (Fennema, 1996). Therefore, some interaction between carboxyl groups of the polyelectrolyte (dispersant) may take place with surface hydroxyls of starch.

A slightly lower relative green density value (60%TD) was achieved for the compacts with starch. A significant degree of swelling and solubilization of starch is expected to occur by prolonged heating at 90 °C for 30 min (Pabst et al., 2002). As the granules incorporate some water, the volume of starch can increase up to a maximum that corresponds to all the available water volume. The starch volume in this study can increase approximately up to a maximum of 2.2–2.8 times. This results is similar to that found by Pabst et al. (2002) and Gregorova and Pabst (2007). Thus, starch volume increased by swelling thereby incorporating additional porosity to the compact volume (Lyckfeldt and Ferreira, 1998).

3.2. *Drying: density and shrinkage of 3Y–ZrO_2 compacts with different amounts of starch*

Fig. 2 shows the volume fraction of starch in the green body (X_{st}) as a function of the volume fraction of added starch, φ. The line in this figure corresponds to the calculated values (Eq. (1)). As φ increased from 0.45 to 0.71 the volume of starch in the green compact increased from 0.27 to 0.65. For low φ values a significant deviation from the calculated X_{st} values could be seen, whereas, for high φ values a good agreement was achieved.

Fig. 3 shows the drying shrinkage versus the volume fraction of starch in the green body. A linear correlation between the shrinkage and X_{st} was found. The shrinkage increased from 4%, for $X_{st} = 0.27$, to 16%, for $X_{st} = 0.65$. Fig. 4 shows the drying shrinkage as a function of the water weight loss of green bodies prepared with different amounts of starch. As

Please cite this article in press as: Garrido, L.B., et al., Effect of starch filler content and sintering temperature on the processing of porous 3Y–ZrO_2 ceramics, J. Mater. Process. Tech. (2008), doi:10.1016/j.jmatprotec.2008.02.074

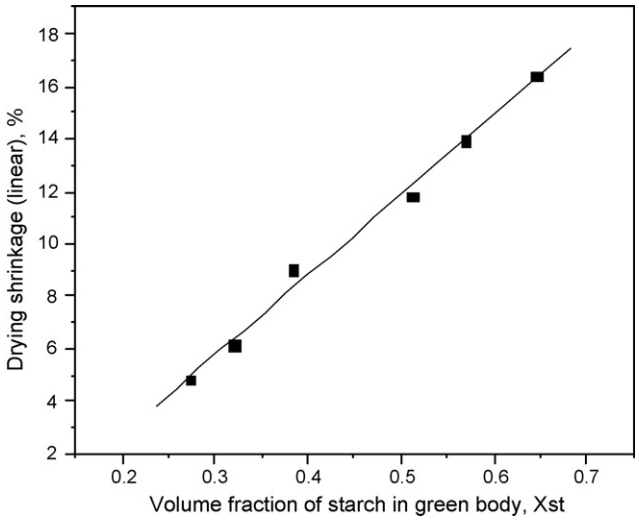

Fig. 3 – Drying shrinkage vs. the volume fraction of starch in the green body.

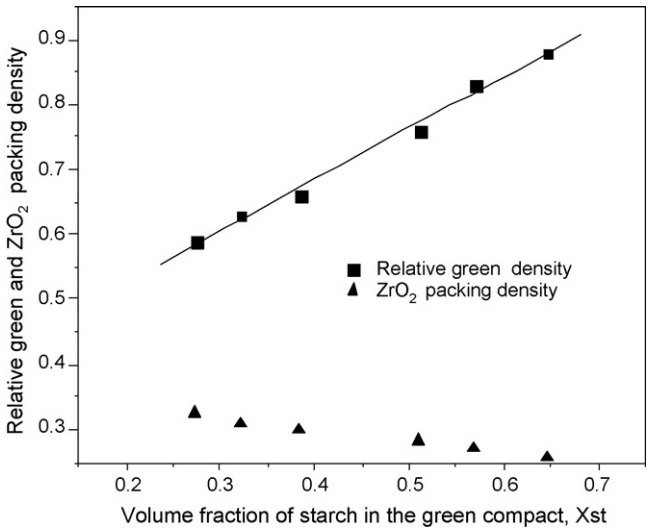

Fig. 5 – Relative density and ZrO_2 packing density vs. the volume fraction of starch in the green compact.

the amount of starch increased, a greater volume of water was required to swell and gel the starch, thereby increasing the water weight loss during drying. The lower water weight loss of the samples with low amounts of starch reduced the drying shrinkage, consequently X_{st} values below the predicted amount were found (Fig. 2). For a given volume of added starch, φ, a high shrinkage decreased the volume of the green compact and consequently increased the X_{st} values. Therefore, for high starch additions the good agreement between the experimental and predicted X_{st} values (Fig. 2) could be explained by an important shrinkage of the green bodies.

Fig. 5 shows the relative density of the green compact and the ZrO_2 packing density versus the volume fraction of starch in the green compact.

The ZrO_2 packing density slightly decreased from 0.325 to 0.257, however, the relative density of the green compacts increased from 0.59, for $X_{st} = 0.27$, to 0.87, for $X_{st} = 0.65$. As an increasing amount of starch is added to the initial composition, more dissolved starch was deposited between and around the zirconia particles, forming a network which reduced the porosity of the body. In addition, a compressive stress on the particle network was probably developed during drying, due to capillary forces on the fluid resulting in a particle packing rearrangement (Barea et al., 2005).

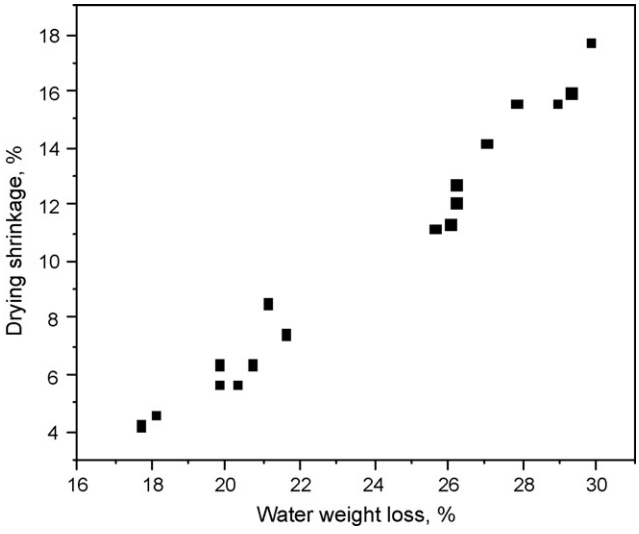

Fig. 4 – Drying shrinkage as a function of the water weight loss of green bodies prepared with different amounts of starch.

3.3. *Starch granules and microstructure of dried compacts*

Fig. 6 shows SEM micrographs of corn starch granules and the fractured surfaces of green compacts with X_{st} of 0.27 and 0.32; the mean granule size was approximately 10 μm. In the microstructure of the dried samples, large spherical cavities, created by the original starch particles, and small voids between the zirconia particles are apparent. Large cavities were uniformly distributed in the compact and had a mean diameter of about 10 μm, which corresponded well to the shape and size of the individual starch particles originally added. Thus, porosity measured in the dried sample consisted of both large spherical cavities formed by drying shrinkage of the starch gel and those of 3Y–ZrO_2 packing. Components of the starch gel network intrude into the 3Y–ZrO_2 matrix region (Pabst et al., 2002), around the space initially occupied by the swollen granule. Further drying caused shrinkage with dehydration of the gelatinized starch. The distribution of starch species during drying is clearly evident by SEM-EDAX analysis of the dried sample. The Zr, C and O mapping are shown in Fig. 7(b–d). Fig. 7c (Yellow points) confirmed the presence of starch deposits, identified as residual C, mainly located in the region around the large cavities.

3.4. *Sintering and shrinkage of samples*

Fig. 8 shows the relative sintered density as a function of the sintering temperature for samples without starch and with

Please cite this article in press as: Garrido, L.B., et al., Effect of starch filler content and sintering temperature on the processing of porous 3Y–ZrO_2 ceramics, J. Mater. Process. Tech. (2008), doi:10.1016/j.jmatprotec.2008.02.074

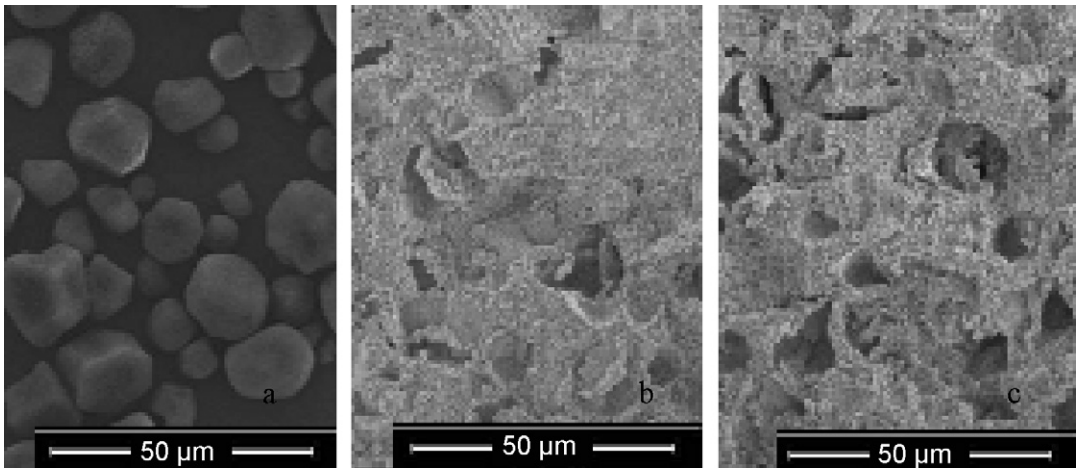

Fig. 6 – SEM micrographs of corn starch granules and fracture surface of dried samples with $X_{st} = 0.27$ and $X_{st} = 0.32$.

X_{st} values of 0.27–0.65. The relative sintered density of casts without starch increased from 0.64 to 0.86, with increasing the sintering temperature from 1000 to 1300 °C, and achieved nearly full densification at 1500 °C.

The relative sintered density of the porous samples, which was significantly lower than that of the samples without starch, increased with increasing the sintering temperature up to 1500 °C, mainly due to the densification of the zirconia matrix.

For the range of X_{st} values studied, the relative sintered density slightly decreased from 0.33 to 0.28 and 0.53 to 0.43, for sintering temperatures of 1000 and 1400 °C, respectively. In the case of bodies with X_{st} of 0.27 and 0.57 sintered at 1000 °C, total porosity reached close to 67% and 72%, respectively. Since densification of 3Y–ZrO_2 began at temperatures above 1000 °C, the porosity created at this temperature corresponded well to the sum of X_{st} and the porosity originally present in the dried compact. At 1400 °C, when matrix densification was significant, porosity of these materials achieved 45 and 66%. At low X_{st}, all pores created by starch were significantly large and do not sinter. Slamovich and Lange (1992) showed that the growth rate of the zirconia matrix grains is slow and therefore do not affect the thermal stability of large pores than grains.

Fig. 9 shows the volumetric sintering shrinkage of the compacts as a function of X_{st} for different sintering temperatures. For each X_{st} value, the increase in the shrinkage with increas-

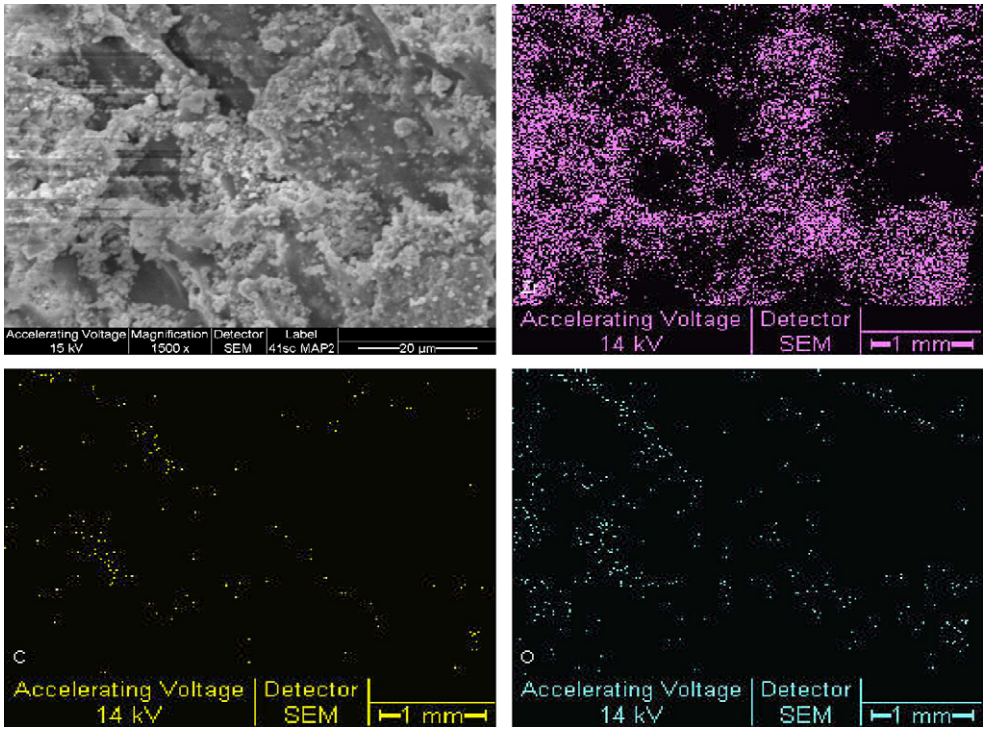

Fig. 7 – SEM-EDAX micrographs of fracture surface of dried 3$YZrO_2$ and Zr, C and O mapping (For interpretation of the references to color in this figure legend, the reader is referred to the web version of the article).

Please cite this article in press as: Garrido, L.B., et al., Effect of starch filler content and sintering temperature on the processing of porous 3Y–ZrO_2 ceramics, J. Mater. Process. Tech. (2008), doi:10.1016/j.jmatprotec.2008.02.074

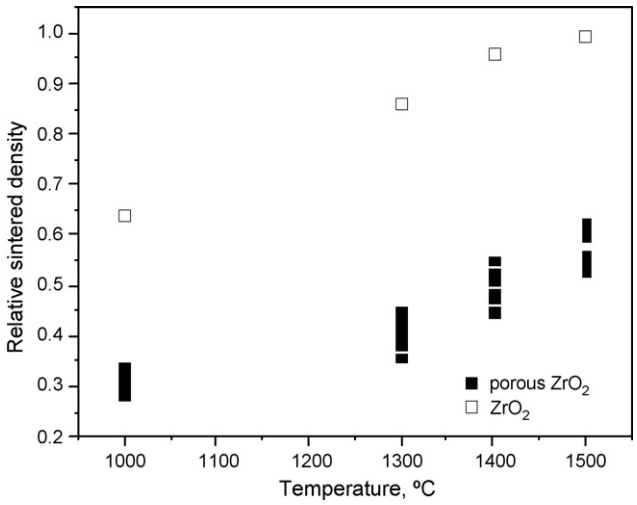

Fig. 8 – Relative sintered density as a function of the sintering temperature for samples without starch and with X_{st} values between 0.27 and 0.65.

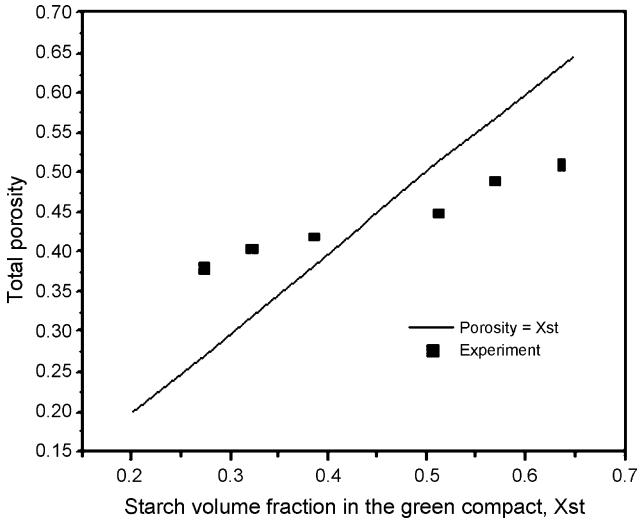

Fig. 10 – Total porosity of the samples sintered at 1500 °C vs. X_{st}.

ing sintering temperature could be attributed to the sintering of the zirconia particles. As the relative green densities of the samples without starch were higher than those with starch the volumetric sintering shrinkage was significantly lower for all the temperatures. However, the samples containing added starch, with X_{st} values from 0.27 to 0.65, had a similar sintering shrinkage. This could be expected since the sintering shrinkage was dependent on the ZrO_2 packing density which slightly reduced for the different X_{st} values (Fig. 5). Thus, the sintering shrinkage exhibited a small dependence on the added starch content.

3.5. *Influence of the volume fraction of starch on the total porosity*

Fig. 10 shows the total porosity of the samples sintered at 1500 °C versus X_{st}; a 1:1 relationship between the bulk porosity and the volume of starch in the green compact was also indicated. This relationship assumed that full densification of the zirconia matrix occurred and consequently the porosity created corresponded to the volume fraction of originally added starch.

The porosity linearly increased with increasing the starch content from 0.35, for $X_{st} = 0.27$, to a maximum value of 0.45, for $X_{st} = 0.65$. For X_{st} lower than 0.4, the total porosity was above the expected amount. In contrast, for X_{st} higher than 0.55, the porosity was lower than that predicted.

For low X_{st} values, the increase in the starch particle volume arising from swelling produced an increase in the size of larger pores, thereby increasing the volume percentage of porosity in the sintered body. Moreover, some voids might also be incorporated by an incomplete mixing or poor dispersion of the starch particles (Lyckfeldt and Ferreira, 1998). For high amounts of added starch, a high percentage of the small pores created by the dissolved starch were eliminated at high sintering temperatures, resulting in a lower porosity than that predicted.

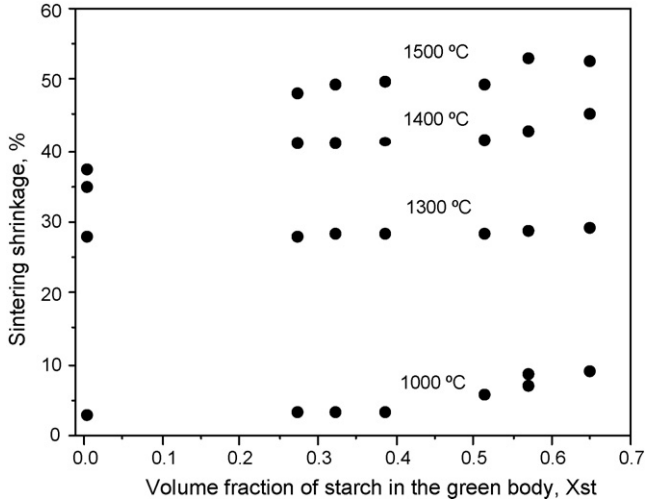

Fig. 9 – Volumetric sintering shrinkage of the compacts as a function of X_{st} for different sintering temperatures.

3.6. *Microstructure of porous materials*

The microstructure shown in Fig. 11 consists of spherical pores, arising from the original starch particles, connected by uniformly distributed channels. The microstructure consists of spherical pores, arising from the original starch particles, connected by uniformly distributed channels. SEM examination of the high porosity material shows examples of shells and cracks surrounding the pores (Fig. 11). These shells were earlier observed by Lyckfeldt and Ferreira (1998) using the starch processing method. Further studies clearly exhibited their presence (Alves et al., 1998) and showed that after burning some of them were completely detached from the matrix (Barea et al., 2005). In addition, a minor amount of micro-cracks were observed located perpendicular to the pore surface, but they were much smaller in size than those surrounding the large pores. The ZrO_2 packing density was low

Please cite this article in press as: Garrido, L.B., et al., Effect of starch filler content and sintering temperature on the processing of porous 3Y–ZrO_2 ceramics, J. Mater. Process. Tech. (2008), doi:10.1016/j.jmatprotec.2008.02.074

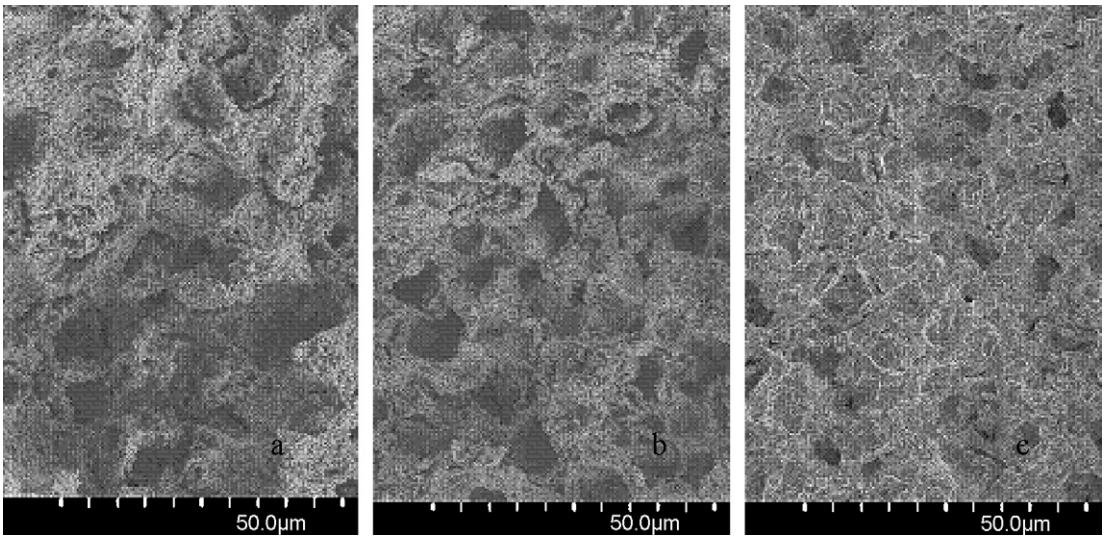

Fig. 11 – SEM micrographs of the fracture surfaces of 50 vol.% porosity ZrO_2: (a) $X_{st} = 0.27$ sintered at 1300 °C, (b) $X_{st} = 0.52$ sintered at 1400 °C and (c) $X_{st} = 0.57$ sintered at 1500 °C.

in the region adjacent to the pore, however, the particles were densely packed in the interior of the matrix where small pores were found. Thus, the region close to the pore shrank more than the interior of the matrix (Deng et al., 2002). Therefore, the shells and cracks surrounding the pores could be attributed to the differential shrinkage between these regions (Lyckfeldt and Ferreira, 1998).

Fig. 12 shows high magnification SEM micrographs of 3Y–ZrO_2 samples with $X_{st} = 0.52$ and $X_{st} = 0.57$, sintered at 1400 and 1500 °C, respectively. As X_{st} and sintering temperature increased, the size of the spherical pores was reduced to 8–9 μm, and the pore shape often changed to one that was more elongated, with a length up to 12 μm.

Fig. 13 shows an SEM image of a sample sintered at 1500 °C, with 50 vol.% porosity, and demonstrates the formation of a polycrystalline grain connection between pore surfaces. According to Suder and Lange (1992) this configuration is thermally unstable, as desintering would likely occur after extended times (i.e. the grain bridge will ultimately disappear). At temperatures lower than 1500 °C, the majority of the grains exhibited a nearly spherical shape and a low volume fraction

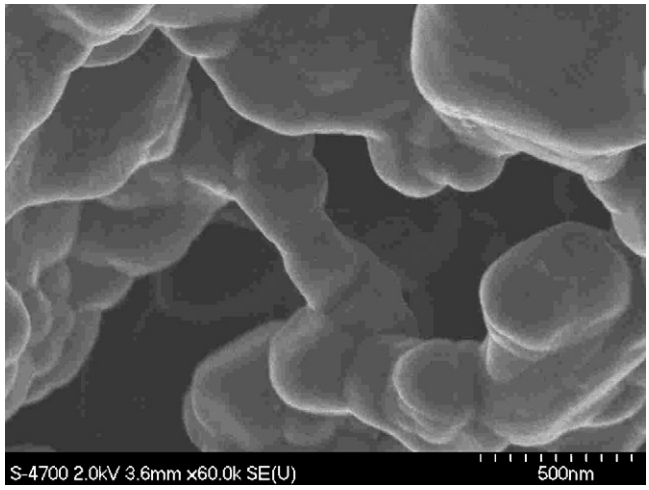

Fig. 13 – High magnification SEM image of a sample sintered at 1500 °C with 50 vol.% porosity.

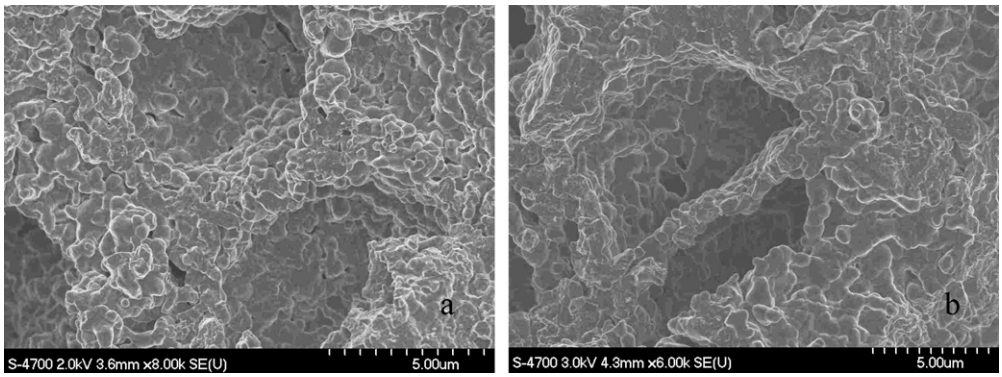

Fig. 12 – SEM micrographs of samples with varying X_{st}: (a) $X_{st} = 0.52$ sintered at 1400 °C and (b) $X_{st} = 0.57$ sintered at 1500 °C.

Please cite this article in press as: Garrido, L.B., et al., Effect of starch filler content and sintering temperature on the processing of porous 3Y–ZrO_2 ceramics, J. Mater. Process. Tech. (2008), doi:10.1016/j.jmatprotec.2008.02.074

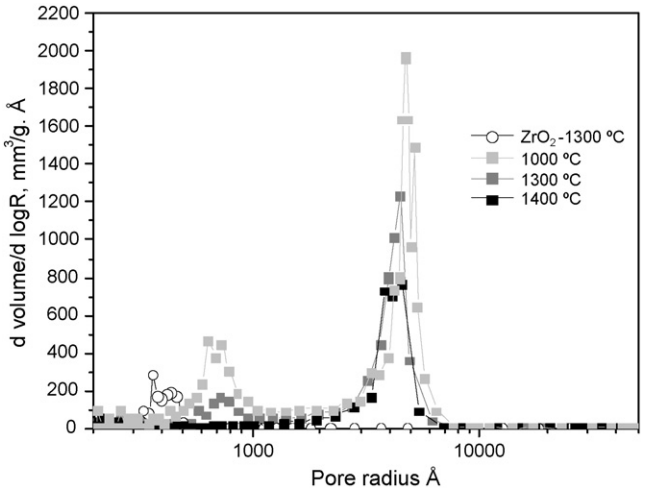

Fig. 14 – Differential pore channel size distribution curves of a zirconia compact with low porosity at different sintering temperatures.

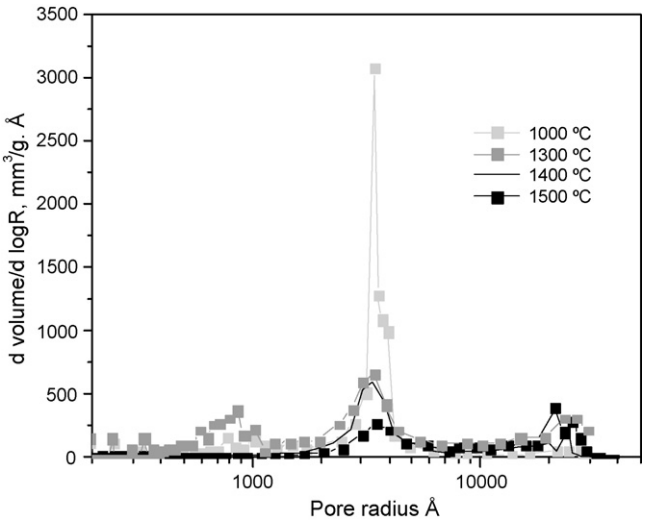

Fig. 15 – Channel size distribution curves of a sample with high porosity sintered at different temperatures.

of isolated porosity remained in the matrix. At 1500 °C the matrix was fully densified, with some elongated pores left by the starch. These pores probably originated at points of interconnection between neighboring starch granules at high X_{st} values. In addition, the fracture of grain connections between opposite surfaces of a crack or defect, as matrix densification proceeded (Suder and Lange, 1992), might contribute to the elongated shape of the pores.

Mercury porosimetry was used to measure the smaller channels which corresponded to the connecting contact areas or necks between larger pores. Fig. 14 shows the differential pore channel size distribution curves of a 3Y–ZrO_2 compact with low porosity, processed at different sintering temperatures. For the samples with starch sintered at 1000 and 1300 °C, a bimodal channel distribution was found. The less frequent mean channel radius was 800–900 Å (channel diameter <0.2 μm) and the most frequent one was 4000–4500 Å (channel diameter <0.9 μm). As the sintering temperature increased to 1400 °C, the volume of the small channels decreased and disappeared completely at 1500 °C. This was due to the development of necks between the zirconia grains at temperatures above 1400 °C. In addition, a reduction in the volume and size of the large channels occurred with increasing sintering temperature.

The pore size of 3Y–ZrO_2, prepared without starch and sintered at 1300 °C, was about 400–500 Å which corresponded to the voids between the zirconia particles. These pores were approximately half the diameter of the small channels in the materials prepared with starch. At 1400 °C the 3Y–ZrO_2 prepared without starch reached essentially complete densification, with only a minor amount of closed porosity remaining.

The channel size distribution curves of a sample with a high starch-derived porosity, sintered at different temperatures are presented in Fig. 15. For the samples sintered at 1000 and 1300 °C, three channel radii existed, the least commonly occurring radii were 800–900 Å and 23500–26500 Å, while the most frequent radius was 3400–3500 Å. The last one was slightly smaller than the most frequent pore size of the low porosity samples. The 800–900 Å channels were removed by sintering at temperatures ≥1400 °C, resulting in a bimodal channel distribution with a low volume of the larger channels.

3.7. *Effect of sintering temperature on open to total porosity ratio*

Fig. 16 shows the open to total porosity ratio versus X_{st} for different sintering temperatures. The porosity was completely open for the samples sintered at 1000 and 1300 °C for the different X_{st} values. This was expected since limited densification of the 3Y–ZrO_2 matrix occurred at these temperatures (Figs. 6 and 7). For sintering temperatures higher than 1300 °C, the open to total porosity ratio increased with increasing X_{st}. For X_{st} = 0.27, open porosity was measurable; there was

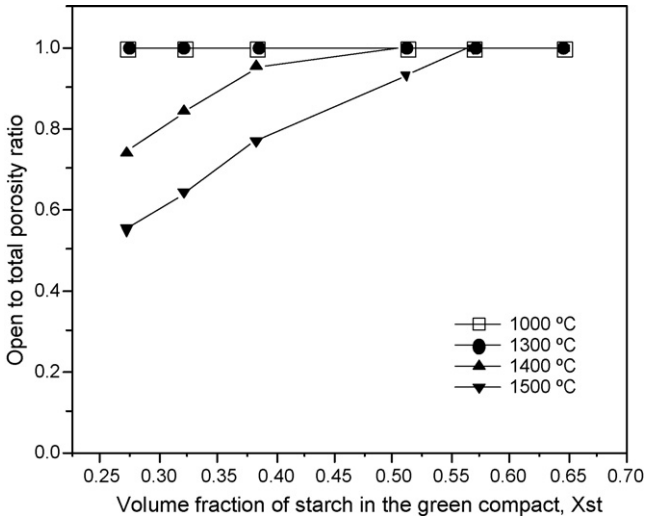

Fig. 16 – Open to total porosity ratio vs. X_{st} for different sintering temperatures.

Please cite this article in press as: Garrido, L.B., et al., Effect of starch filler content and sintering temperature on the processing of porous 3Y–ZrO_2 ceramics, J. Mater. Process. Tech. (2008), doi:10.1016/j.jmatprotec.2008.02.074

a gradual increase in the openness of the pore structure with increasing X_{st} from 0.27 to 0.52 and 0.57, at 1400 and 1500 °C, respectively. This openness could be due to the gradual creation of a percolating starch network within the preform prior to sintering. Thus, the level of interconnectivity between pores increased with increasing starch addition.

4. Conclusions

Porous 3Y–ZrO_2 materials were prepared using starch as a fugitive pore former and binder. The dispersion of 3Y–ZrO_2 particles was not affected by the presence of starch in the suspension. Thus, the maximum relative green density was achieved at nearly the same dispersant concentration for the 3Y–ZrO_2 particles both with and without starch.

The volume fraction of porosity in the sintered compact, which was between 0.48 and 0.65, was dependent on the starch volume fraction in the green body (X_{st}), as well as on the sintering temperature. The porosity increased with increasing the volume of starch in the green body (X_{st}). For $X_{st} < 0.38$, the porosity was higher than that predicted due to swelling of starch granules. For $X_{st} > 0.51$, a high percentage of small pores created by the dissolved starch were eliminated at high temperatures, resulting in a lower porosity than that predicted. At low X_{st}, the microstructure consisted of spherical pores, connected by uniformly distributed channels. As the amount of starch increased, an elongated pore shape appeared due to the interpenetration and overlapping of the starch granules. The porosity was completely open for the samples sintered at 1000 and 1300 °C for all the different X_{st} values, while at 1400 and 1500 °C there was a gradual increase in the openness of the pore structure as X_{st} increased.

REFERENCES

Alves, H.M., Tari, G., Fonseca, A.T., Ferreira, J.M.F., 1998. Processing of porous cordierite bodies by starch consolidation. Mater. Res. Bull. 33, 1439–1448.

Barea, R., Osendi, M., Miranzo, P., Ferreira, J.M.F., 2005. Fabrication of highly porous mullite materials. J. Am. Ceram. Soc. 88, 777–779.

Boaro, M., Vohs, J.M., Gorte, R.J., 2003. Synthesis of highly porous yttria-stabilized zirconia by tape-casting methods. J. Am. Ceram. Soc. 86, 395–400.

Deng, Z.-Y., Yang, J.-F., Beppu, Y., Ando, M., Ohji, T., 2002. Effect of agglomeration of mechanical properties of porous ZrO_2 fabricated by partial sintering. J. Am. Ceram. Soc. 85, 1961–1965.

Deng, Z.-Y., Zhou, Y., Inagaki, Y., Ando, M., Ohji, T., 2003. Role of hard agglomerates in fabricating porous ZrO_2 ceramics and the reinforcing mechanism. Acta Mater. 51, 731–739.

Diaz, A., Hampshire, S., 2004. Characterization of porous silicon nitride produced by starch. J. Eur. Ceram. Soc. 24, 413–419.

Diaz, A., Hampshire, S., Yang, J.-F., Ohji, T., Kanzaki, S., 2005. Comparison of mechanical properties of silicon nitrides with controlled porosities produced by different fabrication routes. J. Am. Ceram. Soc. 88, 698–706.

Fennema, O.R., 1996. Carbohydrates in Food Chemistry. Marcel Dekker, NY, p. 1088.

Gregorova, E., Pabst, W., Bohacenko, I., 2006a. Characterization of different starch types for their application in ceramics processing. J. Eur. Ceram. Soc. 26, 1301–1309.

Gregorova, E., Zivcova, Z., Pabst, W., 2006b. Porosity and pore space characteristics of starch-processed porous ceramics. J. Mater. Sci. 41, 6119–6122.

Gregorova, E., Pabst, W., 2007. Porosity and pore size control in starch consolidation casting of oxides ceramics: achievements and problems. J. Eur. Ceram. Soc. 27, 669–672.

Gu, Y., Liu, X., Meng, G., Peng, D., 1999. Porous YSZ ceramics by water based gelcasting. Ceram. Int. 25, 705–709.

Kim, J.-G., Kwon, Y.-J., Oh, H.-H., Cho, W.-S., Cho, N.-H., Whang, C.-M., Yoo, Y.-C., 2004. Sintering behavior and electrical properties of porous (Ba, Sr)(Ti Sb)O_3 ceramics produced by adding corn starch. Mater. Chem. Phys. 83, 217–221.

Lemos, A.F., Ferreira, J.M.F., 2000. Porous bioactive calcium carbonate implants processed by starch consolidation. Mater. Sci. Eng., c1135.

Luo, J., Stevens, R., 1999. Porosity dependence of elastic moduli and hardness of 3Y–TZP ceramics. Ceram. Int. 25, 281–286.

Lyckfeldt, O., Ferreira, J.M.F., 1998. Processing of porous ceramics by starch consolidation. J. Eur. Ceram. Soc. 18, 131–140.

Pabst, W., Týnová, E., Mikač, J., Gregorová, E., Havrda, J., 2002. A model for the body formation in starch consolidation casting. J. Mater. Sci. Lett. 21, 1101–1103.

Rambo, C.R., Cao, J., Seiber, H., 2004. Preparation of highly porous biomorphic YSZ ceramics. Mater. Chem. Phys. 87, 345–352.

Rosalina, I., Bhattacharya, M., 2002. Dynamic rheological measurements and analysis of starch gels. Carbohydr. Polym. 48, 191–202.

Saggio-Woyansky, R.J., Scott, C.E., Minnear, W.P., 1992. Processing of porous ceramics. Am. Ceram. Soc. Bull. 71, 1674–1682.

Slamovich, S., Lange, F.F., 1992. Densification of large pores. I Experiments. J. Am. Ceram. Soc. 75, 2498–2508.

Studart, A.R., Gonzebach, O.C., Tervoort, E., Gauckler, L.J., 2006. Processing routes to macroporous ceramics: a review. J. Am. Ceram. Soc. 89, 1771–1789.

Suder, O., Lange, F.F., 1992. The effect of inclusions on densification: III desintering phenomenon. J. Am. Ceram. Soc. 75, 3241–3251.

Zender, H., Leistner, H., Searle, H.R., 1990. ZrO_2 materials for application in the ceramic industry. Interceram 39, 33–36.

Please cite this article in press as: Garrido, L.B., et al., Effect of starch filler content and sintering temperature on the processing of porous 3Y–ZrO_2 ceramics, J. Mater. Process. Tech. (2008), doi:10.1016/j.jmatprotec.2008.02.074